
GRIP: GEOMETRIC REFINEMENT AND ADAPTIVE INFORMATION POTENTIAL FOR DATA EFFICIENCY

Changhao Wang*
 Politecnico di Torino
 changhao.wang@polito.it

Jiaolong Yang*
 Ant Group

Xinhao Yao
 Renmin University of China

Yunfei Yu
 Ant Group

Peng Jiao
 Ant Group

Lu Yu
 Ant Group

Junpeng Fang
 Ant Group

Riccardo Cantoro
 Politecnico di Torino

Qing Cui
 Ant Group

Jun Zhou
 Ant Group

ABSTRACT

The performance of Large Language Models (LLMs) is increasingly governed by data efficiency rather than raw scaling volume. However, existing selection methods often decouple global distribution balancing from local instance selection, compromising the hierarchical integrity of the training set. We introduce **GRIP** (Geometric Refinement and Adaptive Information Potential), a framework that unifies these dimensions by modeling the corpus as an information-dense geometric space. GRIP employs a **Rapid Adaptation Probe (RAP)** to quantify the information potential of semantic clusters, dynamically re-allocating the sampling budget to regions with the highest representation deficits. Subsequently, we perform Intra-Cluster Selection using a **length-rectified geometric prior** to counteract embedding density artifacts and preserve long-tail logical sequences. Extensive evaluations on Mixture-of-Experts (MoE) models up to 300B tokens demonstrate that GRIP consistently outperforms state-of-the-art baselines, **surpassing the performance of models trained on $3\times$ larger uncured datasets**. Our work establishes a robust geometric foundation for adaptive data curation in large-scale pre-training.

1 INTRODUCTION

The generalization of Large Language Models (LLMs) has traditionally relied on the simultaneous scaling of model parameters and training data volume (Kaplan et al., 2020). However, current scaling laws suggest that the primary bottleneck for performance has shifted from raw quantity to **data quality** (Hoffmann et al., 2022b; Gadre et al., 2024). As high-quality public corpora approach depletion (Villalobos et al., 2022), simply aggregating noisy web-scale data yields diminishing returns and introduces significant computational waste (Gunasekar et al., 2023; Goyal et al., 2024). This shift necessitates a rigorous focus on **data efficiency**: identifying optimal subsets that maximize information gain per unit of compute (Li et al., 2023; Sorscher et al., 2022).

Recent advances in data efficiency primarily diverge into two paradigms: **structural budgeting** and **instance-level saliency**. The former attempts to balance representational capacity by adjusting mixture weights across predefined domains (Xie et al., 2023a; Liu et al., 2025), yet such coarse-grained adjustments often overlook the underlying semantic cluster and the varying quality within individual clusters (Diao et al., 2025; Wang et al., 2025). In parallel, instance-centric strategies filter data based on difficulty or training dynamics (Zhang et al., 2025b; Wang et al., 2024), but these methods frequently decouple local importance from global topology, inadvertently disrupting the structural coherence essential for complex reasoning. This fragmentation creates a fundamental

*Equal contribution

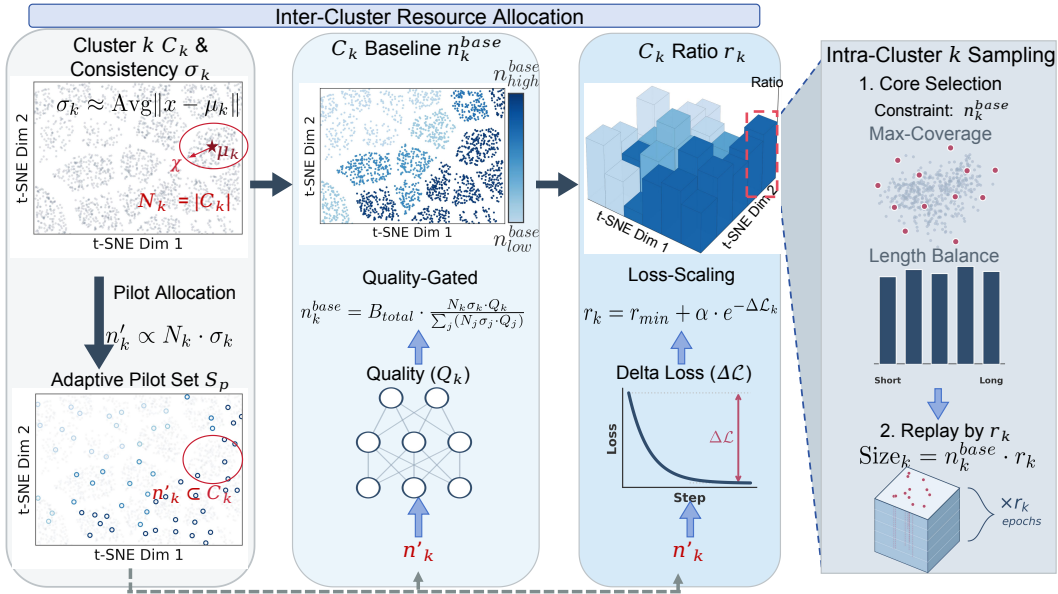


Figure 1: **Overview of the GRIP Framework.** GRIP unifies **Inter-Cluster Budgeting** and **Intra-Cluster Selection** through a hierarchical geometric optimization: **(1) Geometric Probing:** We partition the corpus into semantic clusters and construct a Neyman-optimal probe set \mathcal{P} based on **Geometric Consistency** (σ_k) to estimate the baseline budget n_k^{base} . **(2) Dynamic Allocation:** By monitoring the **Adaptation Delta** ($\Delta\mathcal{L}_k$), GRIP identifies representation deficits and dynamically re-allocates resources from saturated regions to high-potential clusters via a replay multiplier r_k . **(3) Rectified Sampling:** Within clusters, we employ density-based selection with a **Length-Rectification Term** to counteract embedding collapse, preserving both global structural variance and long-tail logical sequences Sorscher et al. (2022); Ethayarajh (2019).

trade-off: current curators either optimize cluster-level proportions while ignoring instance quality, or filter samples while **sacrificing the hierarchical integrity** of the corpus.

This structural integrity is particularly vital for **code corpora**, which form a rigid logical topology defined by brittle syntax and deep hierarchical dependencies (Li et al., 2023; Guo et al., 2020). In code, the loss of rare but structurally critical snippets can degrade the model’s ability to generalize across logical transitions. Furthermore, Transformer embeddings often suffer from a *geometric collapse* in long-context sequences, where high-information samples are suppressed by **density artifacts**, making them difficult to identify via standard filters Ethayarajh (2019); Zhou et al. (2025).

To bridge this gap, we introduce **GRIP** (Geometric Refinement and Adaptive Information Potential), which **unifies inter-cluster budgeting and intra-cluster selection** within an information-dense geometric space. The framework first employs a Rapid Adaptation Probe (RAP) to dynamically re-allocate budgets toward semantic clusters with the highest representation deficits. Subsequently, a **length-rectified geometric prior** is applied for intra-cluster refinement, preserving global structural variance while capturing high-value, long-tail logical sequences to maximize epistemic gain.

We validate GRIP by training 8B and 16B Mixture-of-Experts (MoE) models from scratch, spanning a **training scale from 100B to 300B tokens** on a hybrid corpus. Our results demonstrate that GRIP consistently achieves superior data efficiency and robustness across code generation and reasoning benchmarks compared to state-of-the-art baselines. Our main contributions are:

- **Unified Selection Framework:** We introduce **GRIP**, a hierarchical framework that unifies macro-budgeting with micro-instance selection. Evaluations on MoE architectures up to 300B tokens show that GRIP delivers a significant **+4.6% average improvement** across benchmarks, surpassing the performance of models trained on $3\times$ larger uncurated corpora.
- **Adaptive Information Potential:** We propose the **Rapid Adaptation Probe (RAP)**, a mechanism grounded in \mathcal{V} -usable information theory. RAP identifies “representation deficits” within the

geometric space, enabling **dynamic re-allocation** of the sampling budget based on the model’s evolving epistemic state.

- **Length-Rectified Geometric Selection:** We characterize the **length-induced geometric collapse** in Transformer embeddings and introduce a rectified sampling strategy. This counteracts the suppression of long-context sequences, isolating structurally critical patterns from high-density noise.
- **Loss-Driven Quality Dynamics:** We establish a theoretical link between **instantaneous loss reduction** and **data learnability**. By utilizing training dynamics to reflect intrinsic data quality, our framework prioritizes samples that offer maximum incremental gain throughout the pre-training trajectory.

2 METHODOLOGY

GRIP reformulates data selection as a hierarchical optimization problem over a **structured semantic landscape**, aiming to maximize cumulative information gain within a fixed computational budget. As illustrated in Figure 1, our framework operates across two coupled scales: First, **Inter-Cluster Budgeting** (Sec. 2.3) dynamically calibrates resource allocation by synthesizing intrinsic data quality with the model’s instantaneous learnability. Second, **Intra-Cluster Selection** (Sec. 2.4) employs a length-rectified geometric prior to extract high-value samples, ensuring diverse representation while explicitly counteracting embedding collapse.

2.1 PROBLEM FORMULATION

Let $\mathcal{D} = \{x_i\}_{i=1}^N$ be a large corpus for language-model pretraining. Given a global sampling budget $B_{total} \ll N$, our goal is to extract a support set $S \subset \mathcal{D}$ with $|S| = B_{total}$, such that the information carried by S approximates the full corpus. We measure information through geometry in a representation space: an encoder f_θ maps each sample to a normalized embedding $\mathbf{e}(x) = f_\theta(x) \in \mathbb{S}^{d-1}$. We employ Rao’s quadratic entropy (RQE) (Botta-Dukát, 2005) as the diversity functional, a standard metric in active learning and core-set selection (Sener & Savarese, 2017):

$$\mathcal{I}(\pi) \triangleq \sum_{x,y \in \text{supp}(\pi)} \pi(x) \pi(y) d(\mathbf{e}(x), \mathbf{e}(y)), \quad (1)$$

where π is the sampling distribution. Our optimization objective is to find a sparse distribution π^* that minimizes the divergence from the corpus distribution $\pi_{\mathcal{D}}$:

$$\pi^* = \arg \min_{\pi: |\text{supp}(\pi)|=B_{total}} |\mathcal{I}(\pi) - \mathcal{I}(\pi_{\mathcal{D}})|. \quad (2)$$

We implement this optimization strictly within a hierarchical framework. While matching scalar entropy globally is insufficient to guarantee distributional alignment, applying this criterion locally within the semantic clusters (defined in Sec. 2.2) ensures that the selected subset preserves the local structural variance of the domain, thereby enforcing representational completeness across the entire geometric landscape (Xie et al., 2023b).

2.2 PROBE-CENTRIC REPRESENTATION

Representation Space and Geometric Metrics. To structure the continuous semantic space of \mathcal{D} , we first map each sequence x to a normalized embedding $\mathbf{e}(x) \in \mathbb{S}^{d-1}$ via mean-pooling over the final hidden states of the encoder f_θ . Building upon this representation, we partition the space into K disjoint semantic clusters $\mathcal{C} = \{C_1, \dots, C_K\}$ utilizing spherical k -means (Johnson et al., 2019). Besides, we characterize the geometric property of each cluster C_k by its **Geometric Consistency** σ_k , defined as the root mean square deviation from the centroid μ_k :

$$\sigma_k = \sqrt{|C_k|^{-1} \sum_{x \in C_k} \|\mathbf{e}(x) - \mu_k\|^2}. \quad (3)$$

σ_k quantifies Intra-Cluster Coherence: low values indicate dense semantic alignment (Gao et al., 2021), while high values signal dispersed distributions requiring larger sampling budgets to capture information.

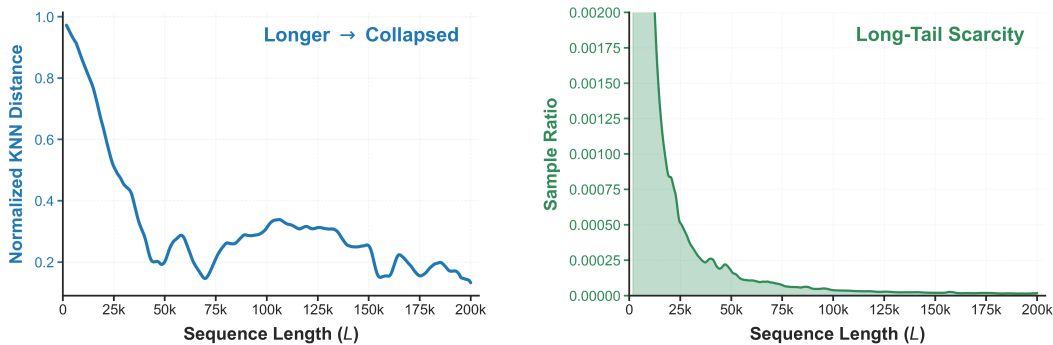


Figure 2: **Analysis of Sequence Length Pathology.** (Left) The normalized distance to the k -nearest neighbors ($k = 10$) decreases rapidly as sequence length grows, indicating that embeddings of long sequences collapse into a narrow, dense region (anisotropic cone). (Right) The sample ratio reveals a severe heavy-tailed imbalance: data density vanishes for long sequences (power-law tail), leading to insufficient supervision for extended contexts.

Neyman-Optimal Probe Construction. To efficiently estimate cluster-level properties (e.g., quality scores Q_k and training dynamics), we construct a lightweight **Probe Set** \mathcal{P} . Instead of uniform sampling, we employ **Neyman’s Optimal Allocation** to minimize the variance of global estimators. We assign the probe budget B_{probe} proportional to the cluster’s size N_k and its geometric dispersion σ_k :

$$n_k^{probe} \propto N_k \cdot \sigma_k, \quad \text{s.t.} \quad \sum n_k^{probe} = B_{probe}. \quad (4)$$

This ensures the probe prioritizes regions with high uncertainty, guaranteeing robust estimation for the subsequent budgeting stage.

The Length-Collapse Pathology. We observe a critical **Length-Induced Embedding Collapse** (Figure 2). As sequences grow, embeddings collapse into a narrow cone, resulting in misleadingly high cosine similarities (pseudo-density) Ethayarajh (2019); Zhou et al. (2025). This structural failure, compounded by the scarcity of long sequences in web corpora (Lozhkov et al., 2024), necessitates the length-aware rectification strategies proposed in Section 2.4.

2.3 INTER-CLUSTER BUDGETING

We formulate data selection as a two-stage allocation problem, distinguishing between **Intrinsic Quality** (static signal-to-noise ratio) and **Instantaneous Learnability** (dynamic information gain). We decouple the allocation into a static *Baseline Budget* and a dynamic *Replay Multiplier*.

Baseline Budget: Static Information Potential. We first allocate the global budget B_{total} to maximize static information coverage. Drawing on **Neural Scaling Laws** (Kaplan et al., 2020; Sorscher et al., 2022), which suggest marginal information gain scales as a power law of data mass, we propose a **Non-Linear Capacity Allocation** rule:

$$n_k^{base} = B_{total} \cdot \frac{(N_k \cdot \sigma_k)^\tau \cdot \exp(Q_k/T)}{\sum_{j=1}^K (N_j \cdot \sigma_j)^\tau \cdot \exp(Q_j/T)}. \quad (5)$$

Here, the sub-linear exponent $\tau < 1$ prevents resource monopolization by massive clusters (Hoffmann et al., 2022a), while the Boltzmann term $\exp(Q_k/T)$ acts as a soft spectral filter, prioritizing high-signal regions (Q_k) estimated by the probe.

Closed-Loop Replay via Loss Dynamics. To align allocation with evolving model capabilities, we leverage the framework of **\mathcal{V} -Usable Information** (Xu et al., 2020; Ethayarajh et al., 2022). We define the utility of cluster C_k as its **Instantaneous Information Potential**—the reduction in entropy achievable given the current feature representation. As illustrated in Figure 3, we estimate

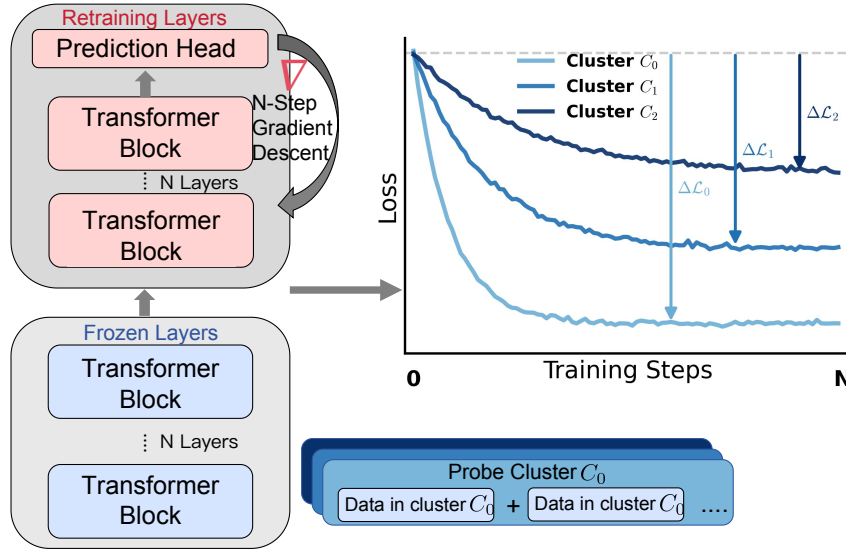


Figure 3: **Mechanism of the Rapid Adaptation Probe.** To evaluate the learnability of different clusters (e.g., C_0, C_1, C_2), we freeze the lower layers and **reset the Retraining Layers to a consistent initialization**. We then perform N -step gradient descent independently for each cluster. The resulting **Adaptation Delta** ($\Delta\mathcal{L}_k$) measures how quickly the loss drops from this common starting point. A rapid loss reduction (e.g., C_0) indicates that the data is easily predictable given the current features, implying low incremental information gain, while a small drop (e.g., C_2) indicates a learning bottleneck requiring increased replay budget.

this via a Rapid Adaptation Probe. We partition the model into **Frozen Layers** (lower transformer blocks) and **Retraining Layers** (upper transformer blocks and prediction head). To ensure a standardized comparison, for each cluster C_k , we reset the Retraining Layers to a shared initialization θ_{init} before performing N -step gradient descent. We then measure the Adaptation Delta:

$$\Delta\mathcal{L}_k = \mathcal{L}(\theta_{init}; C_k) - \mathcal{L}(\theta_N; C_k). \quad (6)$$

Here, $\mathcal{L}(\theta; C_k)$ denotes the loss on cluster C_k given parameters θ . Starting from the same initialization, a rapid loss reduction (large $\Delta\mathcal{L}_k$, e.g., C_0) indicates that the data is easily predictable with current features, implying low incremental information gain. Conversely, a small drop ($\Delta\mathcal{L}_k \rightarrow 0$) signals a **Representation Deficit**, where the model struggles to acquire features. We target these bottlenecks by setting the replay multiplier r_k inversely proportional to the drop:

$$r_k = 1 + \alpha \cdot \exp\left(-\frac{\Delta\mathcal{L}_k}{\tau_{norm}}\right) \cdot \mathbb{I}(Q_k > \tau_{th}). \quad (7)$$

To standardize the learnability signal across varying sequence lengths, we normalize the adaptation delta by its population expectation $\tau_{norm} = \mathbb{E}_k[\Delta\mathcal{L}_k]$. This normalization decouples the metric from scale discrepancies, ensuring it reflects relative information gain. Based on this, the replay intensity is derived inversely to the relative drop, directing the budget toward clusters where the model’s current representation is insufficient. To further refine this objective, we distinguish between valid learnable deficits (epistemic uncertainty) and irreducible noise (aleatoric uncertainty) by strictly coupling the replay intensity with a quality gate $\mathbb{I}(Q_k > \tau_{th})$. This integration ensures that the sampling budget is concentrated on data that is both information-rich and currently underfitted (Qin et al., 2023).

Global Budget Normalization. We synthesize the static capacity and dynamic learnability into a unified **Effective Sampling Utility**, defined as $\mathcal{U}_k^{(t)} = n_k^{base} \cdot r_k^{(t)}$. To adhere to the strict computational constraint B_{total} defined in Eq. 2, we formulate the final allocation using a global partition function $Z^{(t)}$:

$$n_k^{(t)} = \frac{B_{total}}{Z^{(t)}} \cdot \mathcal{U}_k^{(t)}, \quad \text{where } Z^{(t)} = \sum_{j=1}^K \mathcal{U}_j^{(t)}. \quad (8)$$

This renormalization implements a **Zero-Sum Resource Redistribution** (Xie et al., 2023a), automatically siphoning budget from saturated clusters to fund high-deficit regions.

2.4 INTRA-CLUSTER SELECTION

Having established the macro-level budget $n_k^{(t)}$ for each cluster, our final objective is to select specific instances that maximize local geometric coverage. We approach this as a dual-objective sampling problem designed to mitigate semantic redundancy while explicitly counteracting the length-bias pathology inherent in embedding spaces.

Kernel-Based Diversity Sampling. Within a semantic cluster C_k , data points are typically non-uniformly distributed. To enforce **Local Geometric Diversity**, we employ an **Inverse Propensity Sampling** strategy Zhang et al. (2025a). We model the local density $\rho(x)$ of a sample x using a Gaussian Kernel over its nearest neighbors:

$$\rho(x) = \sum_{z \in \mathcal{N}_k(x)} \exp\left(-\frac{\|\mathbf{e}(x) - \mathbf{e}(z)\|^2}{2h^2}\right). \quad (9)$$

We define the base sampling probability as $P_{base}(x) \propto \rho(x)^{-1}$. This mechanism actively penalizes samples located in the dense centroids of the cluster—which typically correspond to common, low-surprisal patterns (Abbas et al., 2023)—and promotes the selection of distinct examples that define the convex hull of the cluster’s semantic span (Tirumala et al., 2023).

Length-Rectified Importance Weighting. Standard density-based sampling fails for long-context data due to the **Length-Induced Collapse** (Sec. 2.2). Since long sequences collapse into a narrow cone, they exhibit artificially high cosine similarities (pseudo-density), causing naive samplers to discard them. To correct this geometric distortion, we introduce a **Length-Rectification Term** β :

$$P_{select}(x) \propto \underbrace{\frac{1}{\rho(x)}}_{\text{Diversity}} \cdot \underbrace{\left(\frac{\ell(x)}{\ell_{avg}}\right)^\beta}_{\text{Length Compensation}}. \quad (10)$$

Here, $\beta \geq 1$ acts as a restoration coefficient. By up-weighting long sequences, we effectively ”re-expand” the collapsed embedding cone (Li et al., 2020). The final subset S_k is drawn from C_k using P_{select} without replacement until the target size $n_k^{(t)}$ is met (Bai et al., 2024).

3 EXPERIMENTAL SETUP

We evaluate **GRIP on large-scale code pre-training**. Code is a demanding setting for data curation: small syntax issues can break execution (Li et al., 2023), the corpus spans many programming languages (Feng, 2020), and programs follow hierarchical dependencies (Guo et al., 2020). These properties make naive filtering brittle, allowing us to strictly test whether GRIP preserves both geometric coverage and local structural integrity.

3.1 CORPUS AND MODEL CONFIGURATION

Hybrid Corpus Composition. To simulate realistic domain augmentation, we construct a **100B token** hybrid candidate pool \mathcal{D}_{pool} comprising a **Fixed Background** (CommonCrawl) and a **Selectable Foreground** (The Stack v2 (Lozhkov et al., 2024)). We employ the *Qwen3 embedding model* Zhang et al. (2025c) to map all candidate documents into a unified dense vector space. Our selection framework operates exclusively on The Stack; the curated high-value subset is then combined with the constant CommonCrawl data to train models from scratch.

Model Architecture. We adopt a fine-grained sparse Mixture-of-Experts (MoE) Transformer, increasing the total expert capacity while keeping the number of activated parameters per token fixed to preserve inference efficiency (Liu et al., 2024). We instantiate **8B** (32 experts) and **16B** (64 experts), both with **1.4B** active parameters. All models are trained **from scratch** with the same training recipe; only the data curation differs

Table 1: **Main Results and Ablation Study.** Comparisons on code generation, reasoning, and multilingual benchmarks. **Panel A** shows scaling efficiency at 300B tokens; **Panel B** details the progressive ablation at 100B tokens. We report **Pass@1** for generation tasks.

Model & Method	Avg. Score	HumanEval		MBPP		LiveCode	CruxEval		MultiPL-E
		Pass@1	HE ⁺	Pass@1	MBPP ⁺	Pass@1	Input	Output	Avg.
<i>Panel A: Scaling Performance (Total Budget: 300B tokens = 100B tokens × 3 Epochs)</i>									
Random 8B	20.2	38.5	36.2	27.4	30.1	1.2	16.5	18.8	13.5
GRIP 8B	24.8 $\uparrow 4.6$	52.4 $\uparrow 13.9$	46.0 $\uparrow 9.8$	36.0 $\uparrow 8.6$	42.6 $\uparrow 12.5$	5.3 $\uparrow 4.1$	24.1 $\uparrow 7.6$	25.8 $\uparrow 7.0$	23.7 $\uparrow 10.2$
Random 16B	20.8	40.8	38.5	29.1	32.5	1.5	18.2	20.4	14.8
GRIP 16B	25.6 $\uparrow 4.8$	55.4 $\uparrow 14.6$	48.2 $\uparrow 9.7$	38.5 $\uparrow 9.4$	44.8 $\uparrow 12.3$	6.4 $\uparrow 4.9$	26.3 $\uparrow 8.0$	26.9 $\uparrow 6.5$	25.5 $\uparrow 10.7$
<i>Panel B: Ablation (GRIP-8B, Total Budget: 100B tokens)</i>									
1. Random	18.7	35.2	32.1	24.5	28.1	0.8	12.5	15.2	11.3
2. + Static Budget	19.4	38.6	35.4	26.2	30.4	1.3	14.4	17.6	13.1
3. + Static Replay	20.2	41.2	38.5	28.1	32.2	1.8	16.3	18.5	14.2
4. + Loss Replay	21.2	44.8	41.5	30.8	34.9	2.4	19.1	20.8	16.5
5. + Diversity	21.3	45.4	42.0	30.5	34.5	2.5	19.3	20.9	16.0
6. GRIP (Full)	22.0 $\uparrow 3.3$	47.2 $\uparrow 12.0$	43.8 $\uparrow 11.7$	32.5 $\uparrow 8.0$	38.2 $\uparrow 10.1$	2.9 $\uparrow 2.1$	20.5 $\uparrow 8.0$	21.8 $\uparrow 6.6$	19.2 $\uparrow 7.9$

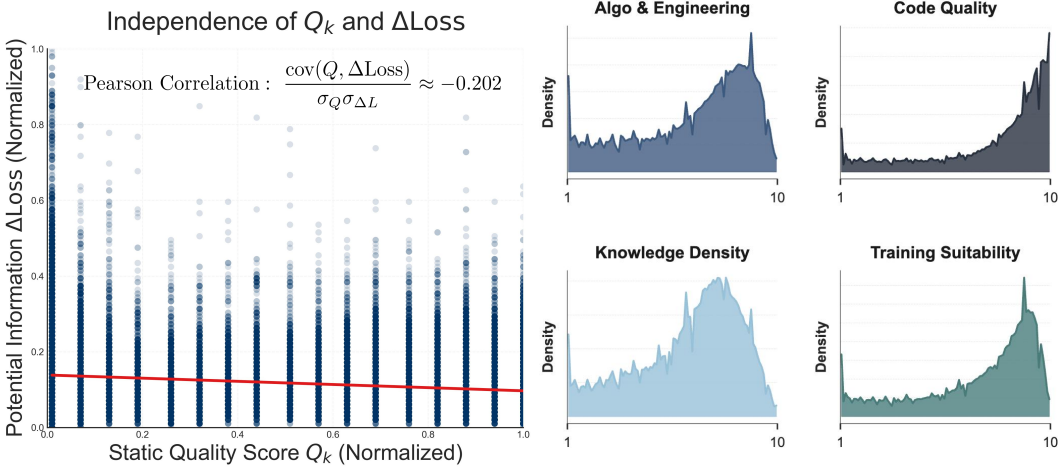


Figure 4: **Independence of Static Quality and Training Dynamics.** (Left) Scatter plot where each data point represents a cluster, showing a weak correlation (Pearson ≈ -0.202) between LLM-based quality scores Q_k and the adaptation delta $\Delta\mathcal{L}_k$. (Right) Density distributions across four dimensions illustrate that high-value semantic features exhibit distinct spectral signatures.

3.2 GRIP IMPLEMENTATION DETAILS

Probe Construction and Static Quality. We construct a Neyman-optimal probe \mathcal{P} ($|\mathcal{P}| \approx 0.5\%$) to serve as a statistical proxy for the corpus. We derive cluster quality Q_k by applying the **LLM-as-a-Judge** paradigm (Zheng et al., 2023) directly to the probe samples using Qwen3-2.35B (Qwen Team, 2025). Documents are scored on educational value and correctness to formulate the aggregate metric Q_k . Exact prompts are detailed in Appendix A.1.

Look-Ahead Dynamics and Loss Calculation. To strictly measure the *learnability* of data clusters rather than mere memorization, we implement a **Parameter Reset Protocol**. For a given probe batch from cluster C_k :

- **Proxy Model Selection:** We utilize **SmolLM-135M** and **360M** as efficient proxies for look-ahead dynamics, while **Qwen-2.5** serves as a larger reference to validate the consistency of learnability rankings.

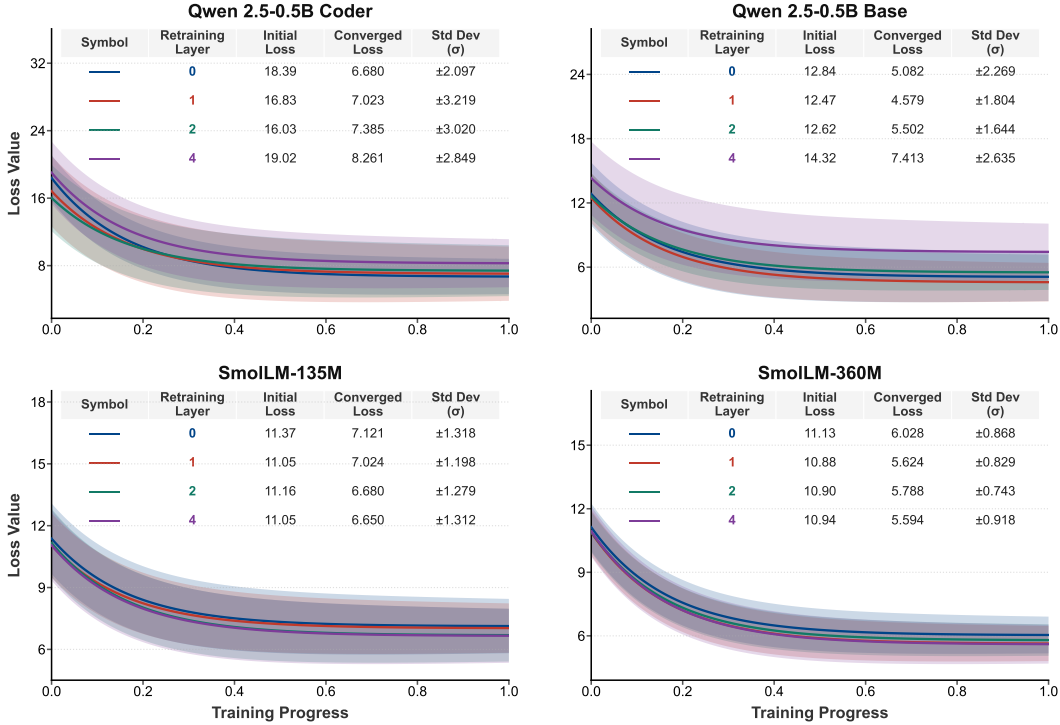


Figure 5: **Cross-Model Transferability of Loss Dynamics.** Loss trajectories across different model families (Qwen-2.5 vs. SmoLLM) and reset depths ($N \in \{0, 1, 2, 4\}$). The high consistency in ranking suggests that lightweight proxy models can effectively guide data selection for larger target architectures.

- **Partial Reset:** We freeze the backbone and re-initialize the weights of the LM head and the last N transformer layers to a random state. We configure the reset depth $N \in \{0, 1, 2, 4\}$.
- **Adaptation Step:** We optimize the reset parameters using AdamW ($\text{lr} = 3 \times 10^{-4}$) and perform $K = 10$ training epochs over the cluster-specific batch to ensure sufficient feature adaptation.
- **Metric Computation:** To decouple the metric from sequence length variations, we normalize the loss by the token count L (length-normalization). We then compute the learnability score as the relative reduction: $\delta\mathcal{L} = (\mathcal{L}_{init} - \mathcal{L}_{final}) / \mathcal{L}_{init}$.

This metric isolates the gradient information gain available to the model given its current representation.

Hyperparameters. We set the probe gradient steps $N = 10$ to efficiently capture the loss convergence *elbow*. In **Dynamic Replay** (Eq. 7), we set the intensity $\alpha = 2.0$ (allowing a max $3\times$ budget). Crucially, to address varying loss magnitudes caused by factors like sequence length, we set the normalization factor $\tau_{norm} \approx \mathbb{E}[\Delta\mathcal{L}]$. This standardizes the adaptation delta, ensuring the replay mechanism responds to relative learnability rather than absolute scale. For **Inter-Cluster Budgeting** (Eq. 5), we adopt square-root sampling ($\tau = 0.5$) to ensure sub-linear scaling, with temperature $T = 1.0$ to preserve the natural quality distribution. Finally, we set the length-penalty $\beta = 0.3$ in **Intra-Cluster Selection** to mitigate embedding collapse. Experiments are conducted on $8\times$ NVIDIA H800 GPUs using AdamW.

3.3 EVALUATION PROTOCOL

Baselines and Ablations. We design a progressive ablation path to verify each component:

- **Random Sampling (Lower Bound):** Uniformly samples tokens from The Stack without any filtering, serving as the baseline for data distribution.

- **Static Quality Budgeting:** Applies only the *Baseline Budget* (n_k^{base} , Eq. 5) based on probe-estimated quality Q_k . This variant ignores training dynamics (Replay) and intra-cluster geometry.
- **Static + Quality-Based Replay:** Introduces a replay mechanism, but calculates the multiplier r_k using static quality scores (Q_k) rather than loss dynamics. This baseline tests whether the *dynamic* nature of our feedback loop is necessary, or if simply up-weighting high-quality static data suffices.
- **Static + Loss-Based Replay (No Diversity):** Incorporates our proposed *Closed-Loop Replay* (Eq. 7) based on $\delta\mathcal{L}$, but employs random sampling within clusters. This isolates the gain from the macro-level budgeting strategy.
- **Static + Loss-Based Replay + Diversity (No Length Fix):** Adds the *Kernel-Based Diversity Sampling* (Eq. 10, first term) but omits the length-rectification term ($\beta = 0$). This validates the specific contribution of our length-aware correction.
- **GRIP (Ours):** The full framework integrating Inter-Cluster Budgeting, Loss-Based Replay, and Length-Rectified Intra-Cluster Selection.

Benchmarks. We evaluate performance across three dimensions:

- **Code Generation:** We utilize *HumanEval(+)* (**HE**) (Chen, 2021) and *MBPP(+)* (Austin et al., 2021) to evaluate generation performance.
- **Robustness & Reasoning:** We assess temporal generalization using *LiveCodeBench* (**LCB**) (Jain et al., 2024) and execution prediction capabilities using *CruxEval* (Gu et al., 2024).
- **Multilingual Proficiency:** We conduct a fine-grained analysis across multiple programming languages using *MultiPL-E* (Cassano et al., 2023).

4 RESULT ANALYSIS

4.1 SCALING EFFICIENCY AND GENERALIZATION

We evaluate the performance of GRIP across two model scales (8B and 16B) to assess its scaling efficiency. As shown in **Table 1 (Panel A)**, GRIP consistently outperforms the random sampling baseline, with the performance gap widening as model capacity increases.

Widening Gains at Scale. GRIP achieves a substantial average score improvement of **+4.6%** on the 8B model, which further expands to **+4.8%** on the 16B architecture. This trend indicates that while random selection suffers from diminishing returns due to noise accumulation, our geometric and learnability-driven strategy effectively saturates the larger model’s capacity with high-information density data, preventing the “data exhaustion” typically seen in scaling.

Superior Reasoning and Robustness. The advantages of GRIP are most pronounced in reasoning-intensive benchmarks, specifically **LiveCodeBench** (+4.1% on 8B) and **MultiPL-E** (+10.2% on 8B). Unlike standard benchmarks that may rely on rote memorization of common patterns, these results demonstrate that GRIP prioritizes data containing complex logical structures and diverse syntax, thereby significantly enhancing the model’s ability to generalize across languages and solve novel algorithmic challenges.

4.2 PROGRESSIVE ABLATION STUDY

To verify the contribution of each component, we analyze the ablation path in **Table 1 (Panel B)**.

- **Efficacy of Static Optimization (Row 1–3):** The transition from Random to **Static Budgeting** (Row 2) delivers a solid initial boost (+0.7% Avg), validating our probe-based strategy for optimizing macro-distributions. Subsequently, adding **Static Replay** (Row 3) yields a further +0.8% gain. These results establish that while prioritizing high-quality (Q_k) data provides a strong foundation, purely static filtering lacks the adaptability to target the model’s evolving information needs.
- **Static vs. Dynamic Replay (Row 3 vs. 4):** Transitioning from static quality budgeting to our **Loss-Based Replay** yields a consistent improvement (**+1.0%** Avg). This confirms that static

heuristics are insufficient for capturing the evolving needs of the model; instead, the instantaneous *learnability* signal ($\Delta\mathcal{L}$) effectively identifies and up-weights "hard-to-learn" clusters that harbor the highest marginal information gain.

- **The "Diversity Trap" (Row 4 vs. 5):** Crucially, applying **Kernel-Based Diversity Sampling** alone results in stagnation (+0.1% Avg) and a notable performance drop in structural tasks like **MultiPL-E** (16.5 \rightarrow 16.0). This reveals a "diversity trap": naive density sampling falls victim to the embedding collapse pathology, erroneously discarding high-value long-context code as redundant, which harms the model's ability to maintain long-range dependencies.
- **Length Rectification (Row 5 vs. 6):** The full GRIP framework, incorporating **Length Rectification**, resolves this pathology and delivers a decisive final boost (+0.7% Avg). By explicitly "re-expanding" the probability mass for collapsed long sequences, we observe a robust recovery in multilingual and reasoning capabilities (e.g., **MultiPL-E** rebounds to 19.2). This validates that geometric diversity is only effective when rectified for the structural biases of the Transformer's representation space.

4.3 VALIDATION OF SELECTION DYNAMICS AND GEOMETRIC ANALYSIS

Independence of Static Quality and Loss Dynamics. As illustrated in Figure 4, we observe a weak correlation (Pearson ≈ -0.202) between static quality Q_k and dynamic learnability $\Delta\mathcal{L}_k$ across semantic clusters. Notably, clusters with near-zero static quality exhibit a wide range of potential information gain, suggesting that even ostensibly "low-quality" data can harbor significant learning utility depending on the model's current state. Furthermore, the density profiles across dimensions—*Algo & Engineering*, *Code Quality*, *Knowledge Density*, and *Training Suitability*—highlight the multi-faceted distribution of high-value data. This independence underscores that static heuristics alone cannot fully capture data importance; integrating dynamic loss feedback is essential to identify incremental information gain relative to the model's evolving representation.

Robustness and Transferability of Proxy-Guided Selection. To strictly decouple intrinsic data learnability from model-specific memorization capacity, we conduct a comprehensive sensitivity analysis using four proxy architectures (SmolLM-135M/360M and Qwen-2.5-0.5B Base/Coder) across varying parameter reset depths $N \in \{0, 1, 2, 4\}$, where $N = 0$ denotes retraining only the prediction head. As illustrated in Figure 5, while stronger architectures like Qwen-Coder exhibit heightened sensitivity to data quality—manifesting in larger adaptation deltas ($\Delta\mathcal{L} \approx 11$) and wider discriminative variance ($\sigma \approx 2.8$) compared to smaller models (e.g., SmolLM-360M: $\Delta\mathcal{L} \approx 5, \sigma \approx 0.8$)—the structural behavior remains remarkably consistent. Crucially, the relative ranking of cluster utility proves robust across both reset depth and model scale: the convergence topologies of ultra-lightweight proxies mirror those of larger reference models, confirming that the learnability signal is an intrinsic geometric property of the data rather than an artifact of training capacity. This dual consistency validates our deployment of the computationally efficient $N = 0$ protocol, which faithfully guides the data budget for the 16B target model with a negligible overhead of less than 1% of total pre-training FLOPs.

Geometric Collapse and Length Rectification. Figure 2 provides empirical confirmation of the embedding pathology targeted by our sampling strategy. The left panel reveals a precipitous decay in normalized k -NN distance—dropping below 0.2 for sequences exceeding 50k tokens—while the right panel highlights the extreme scarcity of such samples in the natural distribution. This intersection creates a "double jeopardy": rare long sequences exhibit artificially high density, causing standard diversity samplers to erroneously discard them as redundant. By implementing length-rectified weighting to counteract this suppression, GRIP ensures adequate supervision for extended contexts, directly contributing to the significant gains observed in complex reasoning benchmarks (e.g., +5.7% on MultiPL-E) where maintaining long-range structural dependencies is critical.

5 CONCLUSION

In this work, we presented **GRIP**, a framework that maximizes data efficiency by treating pre-training as a dynamic semantic space approximation problem. By integrating a rapid adaptation probe to resolve macro-level redundancy and length-rectified sampling to counteract micro-level

geometric collapse, GRIP aligns data allocation with the model’s evolving learning state. Our results on 8B and 16B MoE models demonstrate that prioritizing informative geometry over raw volume enables state-of-the-art performance under fixed computational constraints, providing a scalable path for efficient large-scale curation.

REFERENCES

- Amro Abbas, Kushal Tirumala, Dániel Simig, Surya Ganguli, and Ari S Morcos. Semdedup: Data-efficient learning at web-scale through semantic deduplication. *arXiv preprint arXiv:2303.09540*, 2023.
- Jacob Austin, Augustus Odena, Maxwell Nye, Maarten Bosma, Henryk Michalewski, David Dohan, Ellen Jiang, Carrie Cai, Michael Terry, Quoc Le, et al. Program synthesis with large language models. *arXiv preprint arXiv:2108.07732*, 2021.
- Yushi Bai, Xin Lv, Jiajie Zhang, Yuze He, Ji Qi, Lei Hou, Jie Tang, Yuxiao Dong, and Juanzi Li. Longalign: A recipe for long context alignment of large language models. *arXiv preprint arXiv:2401.18058*, 2024.
- Zoltán Botta-Dukát. Rao’s quadratic entropy as a measure of functional diversity based on multiple traits. *Journal of vegetation science*, 16(5):533–540, 2005.
- Federico Cassano, John Gouwar, Daniel Nguyen, Sydney Nguyen, Luna Phipps-Costin, Donald Pinckney, Ming-Ho Yee, Yangtian Zi, Carolyn Jane Anderson, Molly Q Feldman, et al. Multiple: A scalable and polyglot approach to benchmarking neural code generation. *IEEE Transactions on Software Engineering*, 49(7):3675–3691, 2023.
- Mark Chen. Evaluating large language models trained on code. *arXiv preprint arXiv:2107.03374*, 2021.
- Shizhe Diao, Yu Yang, Yonggan Fu, Xin Dong, Dan Su, Markus Kliegl, Zijia Chen, Peter Belcak, Yoshi Suhara, Hongxu Yin, et al. Climb: Clustering-based iterative data mixture bootstrapping for language model pre-training. *arXiv preprint arXiv:2504.13161*, 2025.
- Kawin Ethayarajh. How contextual are contextualized word representations? comparing the geometry of bert, elmo, and gpt-2 embeddings. *arXiv preprint arXiv:1909.00512*, 2019.
- Kawin Ethayarajh, Yejin Choi, and Swabha Swayamdipta. Understanding dataset difficulty with v-usable information. In *International Conference on Machine Learning*, pp. 5988–6008. PMLR, 2022.
- Z Feng. Codebert: A pre-trained model for program-ming and natural languages. *arXiv preprint arXiv:2002.08155*, 2020.
- Samir Yitzhak Gadre, Georgios Smyrnis, Vaishal Shankar, Suchin Gururangan, Mitchell Wortsman, Rulin Shao, Jean Mercat, Alex Fang, Jeffrey Li, Sedrick Keh, et al. Language models scale reliably with over-training and on downstream tasks. *arXiv preprint arXiv:2403.08540*, 2024.
- Tianyu Gao, Xingcheng Yao, and Danqi Chen. Simcse: Simple contrastive learning of sentence embeddings. *arXiv preprint arXiv:2104.08821*, 2021.
- Sachin Goyal, Pratyush Maini, Zachary C Lipton, Aditi Raghunathan, and J Zico Kolter. Scaling laws for data filtering—data curation cannot be compute agnostic. In *Proceedings of the IEEE/CVF Conference on Computer Vision and Pattern Recognition*, pp. 22702–22711, 2024.
- Alex Gu, Baptiste Rozière, Hugh Leather, Armando Solar-Lezama, Gabriel Synnaeve, and Sida I Wang. Cruxeval: A benchmark for code reasoning, understanding and execution. *arXiv preprint arXiv:2401.03065*, 2024. URL <https://arxiv.org/abs/2401.03065>.
- Suriya Gunasekar, Yi Zhang, Jyoti Aneja, Caio César Teodoro Mendes, Allie Del Giorno, Sivakanth Gopi, Mojan Javaheripi, Piero Kauffmann, Gustavo de Rosa, Olli Saarikivi, et al. Textbooks are all you need. *arXiv preprint arXiv:2306.11644*, 2023.

-
- Daya Guo, Shuo Ren, Shuai Lu, Zhangyin Feng, Duyu Tang, Shujie Liu, Long Zhou, Nan Duan, Alexey Svyatkovskiy, Shengyu Fu, et al. Graphcodebert: Pre-training code representations with data flow. *arXiv preprint arXiv:2009.08366*, 2020.
- Jordan Hoffmann, Sebastian Borgeaud, Arthur Mensch, Elena Buchatskaya, Trevor Cai, Eliza Rutherford, Diego de Las Casas, Lisa Anne Hendricks, Johannes Welbl, Aidan Clark, et al. Training compute-optimal large language models. *arXiv preprint arXiv:2203.15556*, 2022a.
- Jordan Hoffmann, Sebastian Borgeaud, Arthur Mensch, Elena Buchatskaya, Trevor Cai, Eliza Rutherford, Diego de Las Casas, Lisa Anne Hendricks, Johannes Welbl, Aidan Clark, et al. Training compute-optimal large language models. *Advances in Neural Information Processing Systems*, 35:30016–30030, 2022b.
- Naman Jain, King Han, Alex Gu, Wen-Ding Li, Fanjia Yan, Tianjun Zhang, Sida Wang, Armando Solar-Lezama, Koushik Sen, and Ion Stoica. Livecodebench: Holistic and contamination free evaluation of large language models for code. *arXiv preprint arXiv:2403.07974*, 2024.
- Jeff Johnson, Matthijs Douze, and Hervé Jégou. Billion-scale similarity search with FAISS. *IEEE Transactions on Big Data*, 2019.
- Jared Kaplan, Sam McCandlish, Tom Henighan, Tom B Brown, Benjamin Chess, Rewon Child, Scott Gray, Alec Radford, Jeffrey Wu, and Dario Amodei. Scaling laws for neural language models. *arXiv preprint arXiv:2001.08361*, 2020.
- Bohan Li, Hao Zhou, Junxian He, Mingxuan Wang, Yiming Yang, and Lei Li. On the sentence embeddings from pre-trained language models. *arXiv preprint arXiv:2011.05864*, 2020.
- Raymond Li, Loubna Ben Allal, Yangtian Zi, Niklas Muennighoff, Denis Kocetkov, Chenghao Mou, Marc Marone, Christopher Akiki, Jia Li, Jenny Chim, et al. Starcoder: may the source be with you! *arXiv preprint arXiv:2305.06161*, 2023.
- Aixin Liu, Bei Feng, Bin Wang, Bingxuan Wang, Bo Liu, Chenggang Zhao, Chengqi Deng, Chong Ruan, Damai Dai, Daya Guo, et al. Deepseek-v2: A strong, economical, and efficient mixture-of-experts language model. *arXiv preprint arXiv:2405.04434*, 2024.
- Fengze Liu, Weidong Zhou, Binbin Liu, Zhimiao Yu, Yifan Zhang, Haobin Lin, Yifeng Yu, Bingni Zhang, Xiaohuan Zhou, Taifeng Wang, et al. Quadmix: Quality-diversity balanced data selection for efficient llm pretraining. *arXiv preprint arXiv:2504.16511*, 2025.
- Anton Lozhkov, Raymond Li, Loubna Ben Allal, Federico Cassano, Joel Lamy-Poirier, Nouamane Tazi, Ao Tang, Dmytro Pykcz, Ben Liu, et al. Starcoder 2 and the stack v2: The next generation. *arXiv preprint arXiv:2402.19173*, 2024.
- Ziheng Qin, Kai Wang, Zangwei Zheng, Jianyang Gu, Xiangyu Peng, Zhaopan Xu, Daquan Zhou, Lei Shang, Baigui Sun, Xuansong Xie, et al. Infobatch: Lossless training speed up by unbiased dynamic data pruning. *arXiv preprint arXiv:2303.04947*, 2023.
- Qwen Team. Qwen3 technical report. *arXiv preprint arXiv:2505.09388*, 2025. URL <https://arxiv.org/abs/2505.09388>.
- Ozan Sener and Silvio Savarese. Active learning for convolutional neural networks: A core-set approach. *arXiv preprint arXiv:1708.00489*, 2017.
- Ben Sorscher, Robert Geirhos, Shashank Shekhar, Surya Ganguli, and Ari Morcos. Beyond neural scaling laws: beating power law scaling via data pruning. *Advances in Neural Information Processing Systems*, 35:19523–19536, 2022.
- Kushal Tirumala, Daniel Simig, Armen Aghajanyan, and Ari S Morcos. D4: Improving llm pre-training via document de-duplication and diversification. In *NeurIPS*, 2023.
- Pablo Villalobos et al. Will we run out of data? an analysis of the limits of scaling datasets in machine learning. *arXiv preprint arXiv:2211.04325*, 2022.

-
- Jiachen T Wang, Dawn Song, James Zou, Prateek Mittal, and Ruoxi Jia. Capturing the temporal dependence of training data influence. *arXiv preprint arXiv:2412.09538*, 2024.
- Jiachen T Wang, Tong Wu, Kaifeng Lyu, James Zou, Dawn Song, Ruoxi Jia, and Prateek Mittal. Can small training runs reliably guide data curation? rethinking proxy-model practice. *arXiv preprint arXiv:2512.24503*, 2025.
- Sang Michael Xie, Hieu Pham, Xuanyi Dong, Nan Du, Hanxiao Liu, Yifeng Lu, Percy S Liang, Quoc V Le, Tengyu Ma, and Adams Wei Yu. Doremi: Optimizing data mixtures speeds up language model pretraining. In *NeurIPS*, 2023a.
- Sang Michael Xie, Shibani Santurkar, Tengyu Ma, and Percy S Liang. Data selection for language models via importance resampling. *Advances in Neural Information Processing Systems*, 36: 34201–34227, 2023b.
- Yilun Xu, Shengjia Zhao, Jiaming Song, Russell Stewart, and Stefano Ermon. A theory of usable information under computational constraints. *arXiv preprint arXiv:2002.10689*, 2020.
- Chi Zhang, Huaping Zhong, Kuan Zhang, Chengliang Chai, Rui Wang, Xinlin Zhuang, Tianyi Bai, Qiu Jiantao, Lei Cao, Ju Fan, Ye Yuan, Guoren Wang, and Conghui He. Harnessing diversity for important data selection in pretraining large language models. In *The Thirteenth International Conference on Learning Representations*, 2025a. URL <https://openreview.net/forum?id=bMC1t7eLRc>.
- Jia Zhang, Chen-Xi Zhang, Yao Liu, Yi-Xuan Jin, Xiao-Wen Yang, Bo Zheng, Yi Liu, and Lan-Zhe Guo. D3: Diversity, difficulty, and dependability-aware data selection for sample-efficient llm instruction tuning. *arXiv preprint arXiv:2503.11441*, 2025b.
- Yanzhao Zhang, Mingxin Li, Dingkun Long, Xin Zhang, Huan Lin, Baosong Yang, Pengjun Xie, An Yang, Dayiheng Liu, Junyang Lin, et al. Qwen3 embedding: Advancing text embedding and reranking through foundation models. *arXiv preprint arXiv:2506.05176*, 2025c.
- Lianmin Zheng, Wei-Lin Chiang, Ying Sheng, Siyuan Zhuang, Zhanghao Wu, Yanping Zhuang, Zi Lin, Zhuohan Li, Dacheng Li, Eric Xing, et al. Judging llm-as-a-judge with mt-bench and chatbot arena. In *Advances in Neural Information Processing Systems*, volume 36, pp. 4659–4675, 2023.
- Yuqi Zhou, Sunhao Dai, Zhanshuo Cao, Xiao Zhang, and Jun Xu. Length-induced embedding collapse in plm-based models. In *Proceedings of the 63rd Annual Meeting of the Association for Computational Linguistics (Volume 1: Long Papers)*, pp. 28767–28791, 2025.

A APPENDIX

A.1 PROMPTS FOR STATIC QUALITY ASSESSMENT

To ensure the selected code data meets rigorous pre-training standards, we employ an **LLM-as-a-Judge** paradigm. Unlike generic scoring, we utilize a specialized "Senior Technical Auditor" persona designed to penalize non-functional code while rewarding pedagogical value and engineering robustness. The full system instruction is provided below.

System Instruction: Comprehensive Code Audit Protocol

You are acting as a **Senior Technical Auditor**. Your objective is to rigorously evaluate the provided code snippet against four core performance indicators.

Unlike simple correctness checks, you must assess the code's readiness for high-quality pre-training datasets. Use a granular **0 to 10 scale** for each dimension.

1. Code Quality & Compliance (0-10)

Focus: Syntax, naming, and readability.

- **0-3 (Low):** Severe syntax errors; code cannot run; messy formatting or naming makes it unreadable.
- **4-7 (Mid):** Executable and generally correct; minor formatting issues or inconsistent naming; readable but not polished.
- **8-10 (High):** Error-free and standard compliant (e.g., PEP8); precise naming; clean and professional structure.

2. Algorithmic & Engineering Design (0-10)

Focus: Modularity, robustness, and structure.

- **0-3 (Low):** All code in one block (global scope); no functions/classes; lacks input validation or error handling.
- **4-7 (Mid):** Split into functions; basic error checking; logic is structured but lacks extensibility.
- **8-10 (High):** High modularity (classes/functions); robust error handling; follows best engineering practices.

3. Training Suitability (0-10)

Focus: Educational value and clarity for learning.

- **0-3 (Low):** No comments; confusing logic; uses "magic numbers"; hard for a model or human to learn from.
- **4-7 (Mid):** Clear logic; includes basic comments for key steps; suitable for general training.
- **8-10 (High):** Excellent comments explaining the "why"; demonstrates best practices; highly suitable for fine-tuning/teaching.

4. Knowledge Density (0-10)

Focus: Technical insight and complexity.

- **0-3 (Low):** Trivial code (e.g., simple print statements, basic loops); contains little domain knowledge.
- **4-7 (Mid):** Standard algorithms or typical business logic; useful but not unique.
- **8-10 (High):** complex algorithms, deep optimizations, or cross-domain knowledge; high technical value.

Response Requirement: Analyze the input code and output a JSON object strictly adhering to this schema:

```
{
  "syntax_integrity_score": <int 0-10>,
  "architecture_score": <int 0-10>,
  "educational_value_score": <int 0-10>,
  "technical_depth_score": <int 0-10>
}
```

Target Code Snippet: \$content